International Journal of Nanomedicine

Dovepress
open access to scientific and medical research

Open Access Full Text Article

ORIGINAL RESEARCH

Brain microvascular endothelial cell association and distribution of a 5 nm ceria engineered nanomaterial

This article was published in the following Dove Press journal:
International Journal of Nanomedicine
26 July 2012
Number of times this article has been viewed

Mo Dan[1,2]
Michael T Tseng[3]
Peng Wu[4]
Jason M Unrine[5]
Eric A Grulke[4]
Robert A Yokel[1,2]

[1]Department of Pharmaceutical Sciences, College of Pharmacy, [2]Graduate Center for Toxicology, University of Kentucky, Lexington, KY, USA; [3]Departments of Anatomical Sciences and Neurobiology, University of Louisville, Louisville, KY, USA; [4]Chemical and Materials Engineering Department, [5]Department of Plant and Soil Science, University of Kentucky, Lexington, KY, USA

Purpose: Ceria engineered nanomaterials (ENMs) have current commercial applications and both neuroprotective and toxic effects. Our hypothesis is that ceria ENMs can associate with brain capillary cells and/or cross the blood–brain barrier.

Methods: An aqueous dispersion of ~5 nm ceria ENM was synthesized and characterized in house. Its uptake space in the Sprague Dawley rat brain was determined using the in situ brain perfusion technique at 15 and 20 mL/minute flow rates; 30, 100, and 500 µg/mL ceria perfused for 120 seconds at 20 mL/minute; and 30 µg/mL perfused for 20, 60, and 120 seconds at 20 mL/minute. The capillary depletion method and light and electron microscopy were used to determine its capillary cell and brain parenchymal association and localization.

Results: The vascular space was not significantly affected by brain perfusion flow rate or ENM, demonstrating that this ceria ENM did not influence blood–brain barrier integrity. Cerium concentrations, determined by inductively coupled plasma mass spectrometry, were significantly higher in the choroid plexus than in eight brain regions in the 100 and 500 µg/mL ceria perfusion groups. Ceria uptake into the eight brain regions was similar after 120-second perfusion of 30, 100, and 500 µg ceria/mL. Ceria uptake space significantly increased in the eight brain regions and choroid plexus after 60 versus 20 seconds, and it was similar after 60 and 120 seconds. The capillary depletion method showed 99.4% ± 1.1% of the ceria ENM associated with the capillary fraction. Electron microscopy showed the ceria ENM located on the endothelial cell luminal surface.

Conclusion: Ceria ENM association with brain capillary endothelial cells saturated between 20 and 60 seconds and ceria ENM brain uptake was not diffusion-mediated. During the 120-second ceria ENM perfusion, ceria ENM predominately associated with the surface of the brain capillary cells, providing the opportunity for its cell uptake or redistribution back into circulating blood.

Keywords: ceria engineered nanomaterial, brain microvascular endothelial cell association, in situ brain perfusion, capillary depletion

Introduction

Commercial and scientific interest in ceria engineered nanomaterials (ENMs) has expanded rapidly in recent years. Numerous studies have found ceria to be neuroprotective, suggesting that it has utility in medical disorders caused by reactive oxygen species.[1–6] In retinal neurons, 5 nm ceria ENM inhibited H_2O_2-induced reactive oxygen species.[7] Ceria ENMs enhanced spinal neuron viability [3] and protected a mixed culture of cortical neurons and glial cells from H_2O_2-induced injury.[8] A protective effect of ceria ENMs on mouse hippocampal slices was demonstrated in a model of ischemia.[5] Although these reports showed the therapeutic potential of ceria ENM as a neuroprotective agent, none has investigated the ability of ceria ENMs to associate with

Correspondence: Mo Dan
Department of Pharmaceutical Sciences, College of Pharmacy, Biopharmaceutical Complex (College of Pharmacy) Building, 789 S Limestone, University of Kentucky Academic Medical Center, Lexington, KY 40536-0596, USA
Tel +1 859 257 2572
Fax +1 859 257 7564
Email mo.dan@uky.edu

and/or cross the blood–brain barrier (BBB). Other studies have found that ceria ENMs can cause oxidative stress and induce toxicity.[9–11] In light of the potential neuroprotective therapeutic applications and toxicity concerns of ceria ENMs, it is very important to understand their interaction with the BBB and brain parenchyma.

Brain capillary endothelial cells cooperate with pericytes, astrocytes, and neurons to generate and maintain the unique barrier properties of the BBB, which plays a crucial role in safeguarding the brain from endogenous and exogenous compounds circulating in the blood.[12] Although the BBB is a tightly regulated barrier, ENMs are being extensively investigated as an approach to deliver drugs to the central nervous system, based on their unique physicochemical properties, such as tight junction disruption, increased retention at the brain capillaries combined with adsorption to the capillary walls, and receptor-mediated transcytosis.[13,14] Several studies have indicated that metal ENMs altered BBB integrity and increased its permeability, and/or led to toxicity to the BBB and the brain.[15,16] The biodistribution of 15, 50, 100, and 200 nm gold nanoparticles was investigated 24 hours after its intravenous (IV) administration. The 15 and 50 nm gold crossed the BBB and entered the brain; the larger ENMs did not.[17] After oral gavage, 25 nm ceria appeared in the brain one day later and was still present in the brain on day 7.[18] Although these studies indicated that some metal oxide ENMs have the potential to cross the BBB, most studies on brain ENM uptake did not separate the capillary endothelial cells from the brain cells, making it difficult to determine whether the ENMs entered the brain or if their distribution was limited to the capillary endothelial cells. More research is needed in order to understand the distribution of ENMs between capillary endothelial cells and/or brain tissue.

Our previous findings showed that 5 nm ceria ENM agglomerates in the brain capillary lumen. Electron microscopy (EM) did not reveal ceria ENM inside microvascular endothelial or brain cells. Ceria did not produce profound pro- or antioxidant effects in the brain one or 20 hours after a 1-hour systematic IV infusion.[19] The reasons for the lack of ceria ENMs in the brain are unknown. One possibility is that the ceria ENMs were rapidly coated by proteins in the blood that changed their physicochemical properties, resulting in their rapid clearance by the mononuclear phagocyte system.[20,21] Another possibility is that the nanoparticles agglomerated very rapidly in the blood or on a biological surface, changing their distribution and cell interaction,[22–25] so that the agglomerated ceria became too large or unavailable to penetrate the intact BBB. The present study utilized a controlled system to better understand how ceria ENMs interact with brain capillary endothelial cells. The results are relevant to the therapeutic use and toxicological consideration of ceria ENMs.

The objective of this study was to investigate the brain capillary cell association and brain entry rate of a 5 nm ceria ENM. We used the in situ brain perfusion method to evaluate BBB integrity and determine brain entry rate at different perfusion flow rates, ceria ENM concentrations, and perfusion durations. Eight brain regions and a choroid plexus (ipsilateral to the perfusion) were collected to test regional differences in BBB integrity and ceria ENM brain entry rate. The capillary depletion method was used to evaluate ceria ENM distribution between capillary and brain tissues. Light microscopy (LM) and EM were used to investigate the localization of ceria nanoparticles.

Materials and methods

Nanomaterial

The 5 nm ceria ENM was synthesized using a previously reported method (supplementary materials).[19] The physicochemical properties of the ceria ENMs were determined in our laboratories. All of the methods have been reported previously (supplementary material).[26] Free cerium in the ceria ENM dispersion was removed by ultrafiltration, using 3 kDa molecular weight cutoff regenerated cellulose centrifugal filtration devices (Amicon Ultra-4; EMD Millipore, Billerica, MA). The 5 nm ceria (3.5 mL) was added to the Amicon Ultra filter unit. The unit was centrifuged at 4800 g for 35 minutes to obtain 3 mL filtrate and 0.5 mL concentrated ceria ENM. The 3 mL filtrate (containing free cerium) was removed from the centrifuge tube, and 3 mL sodium citrate (0.17 M) solution was added to the filtration device to disperse the ceria ENM. After conducting this washing procedure three times, sodium citrate solution (3 mL; 0.17 M) was added to the filtration device, which was bath sonicated for 15 minutes to redisperse the ceria ENM. The Ce concentrations of the 5 nm ceria ENM dispersion and free cerium in the ultrafiltrate were analyzed by inductively coupled plasma mass spectrometry (ICP-MS).[19,26]

Perfusate for in situ brain perfusion

The perfusate contained 30, 100, or 500 μg/mL ceria ENM in a solution of Na^+ (153 mM), K^+ (4.2 mM), Ca^{2+} (1.5 mM), Mg^{2+} (0.9 mM), Cl^- (162 mM), and glucose (9 mM). Gadolinium-diethylenetriamine pentaacetic acid (Gd-DTPA) (1 mM) was added to determine BBB integrity. It has been

shown that Gd-DTPA, a marker for vascular space, does not significantly cross the intact BBB, due to its charge and high molecular weight.[27] A significant increase of Gd-DTPA in brain samples indicates BBB damage. Following at least 1-hour incubation at 37°C, the perfusate was bubbled for 2 minutes with 95/5 air/CO_2 and adjusted to pH 7.4 prior to its use.[28]

Ceria ENM stability in the perfusate

Ceria ENM stability in the perfusate was determined from 1 to 230 minutes (after addition to perfusate) using dynamic light scattering (90Plus Nanoparticle Size Distribution Analyzer; Brookhaven Instruments Corp, Holtsville, NY). The intensity-weighted hydrodynamic diameter in the perfusate was measured at 1000 µg/mL at 37°C, and then it was converted to number- and volume-weighted averages.

Animals

In this study, 55 male Sprague Dawley rats were used, weighing 330 ± 35 g (mean ± standard deviation [SD]). Prior to the study, the animals were housed individually in the University of Kentucky Division of Laboratory Animal Resources Facility. Animal work was approved by the University of Kentucky Institutional Animal Care and Use Committee (Protocol 2008-0272). The research was conducted in accordance with the Guiding Principles in the Use of Animals in Toxicology.

In situ brain perfusion methods

We employed the modification of the brain perfusion technique as previously reported.[28–30] Briefly, the rat was anesthetized under ketamine/xylazine anesthesia (75 and 5 mg/kg), and its left carotid artery was exposed. Following ligation of the external carotid, occipital, and common carotid arteries, PE60 tubing containing heparin (100 U/mL, in 0.9% NaCl) was inserted into the common carotid. We used the heart-cut modification of this technique and increased the perfusate flow rate to 20 mL/minutes.[31] The rat was decapitated to end the perfusion, and the brain was harvested and cleaned of meninges and surface vessels. Brain tissue (~20 mg from each brain region, except the choroid plexus, which averaged 0.9 ± 0.4 mg) was collected from the frontal cortex, parietal cortex, occipital cortex, thalamus/hypothalamus, midbrain/colliculus, striatum, cerebellum, hippocampus, and choroid plexus, from the left hemisphere, for measurement of Gd-DTPA (as gadolinium) and ceria ENM (as cerium) by ICP-MS. Cerebrovascular washout of the perfusate was conducted to test the influence of ceria concentrations in the vascular space on the brain uptake space. The cerebrovascular space was washed at the same perfusion rate (n = 4 rats) for 20 seconds, with ceria-free perfusate, immediately following 100 µg ceria ENM/mL perfusion for 120 seconds at 20 mL/minute. The results were compared to those obtained without cerebrovascular washout, using a two-way analysis of variance (ANOVA). The brain uptake space in the washout and nonwashout conditions did not show a significant difference after correcting for the vascular volume. Therefore, washouts were not conducted in the rest of the studies, except for the capillary depletion experiment, and three rats perfused for LM and EM examination.

Flow-rate-dependent uptake is a property of some carrier-mediated uptake systems, but it is not a property of diffusion.[28] Therefore, to examine the effect of perfusion flow rate on influx rate and the vascular and brain extracellular fluid volumes, 15 and 20 mL/minute flow rates (100 µg ceria ENM/mL) were tested in four and five rats, respectively. To determine whether ceria ENM brain entry is concentration-dependent, three ceria ENM concentrations (30, 100, and 500 µg/mL) were investigated, using a perfusion rate of 20 mL/minute for 120 seconds (n = 4, 6, and 5 rats, respectively). Ceria ENM brain entry during the different perfusion durations was investigated to determine how fast ceria ENM associates with brain capillary cells or enters the brain. Perfusion durations of 20, 60, and 120 seconds, using a rate of 20 mL/minutes and 30 µg ceria ENM/mL were studied in 4 treated animals and 3 control animals in each group. Three animals were prepared for LM and EM after perfusion with 100 µg ceria ENM/mL, 20 mL/minute for 120 seconds, followed by a 20-second washout with ceria-free perfusate.

Capillary depletion method

The capillary depletion method was used to separate brain parenchyma from capillary tissue.[28,32] After a 30-µg/mL, 120-second, 20-mL/minute ceria ENM perfusion, a 20-second washout was conducted. The forebrain from the perfused hemisphere was isolated from 10 rats (2 control and 8 treated), and the lateral ventricle choroid plexus in the perfused hemisphere was removed. The tissue was homogenized in 3.5 mL physiological buffer containing 141 mM NaCl, 4 mM KCl, 2.8 mM $CaCl_2$, 1 mM NaH_2PO_4, 1 mM $MgSO_4$, 10 mM glucose, and 10 mM HEPES at pH 7.4. Dextran (70,000 g/mol) was then added to 18% (w/v), and the sample was further briefly homogenized. After centrifugation at 5400 x g for 15 minutes at 4 °C, the supernatant (brain-rich fraction) and pellet (capillary-rich fraction) were carefully

separated for measurement of ceria ENM by ICP-MS. The percentage of the forebrain ceria ENM in the capillary-rich fraction = (mass amount of cerium in the capillary-rich fraction/mass amount of cerium in the capillary-rich fraction + brain-rich fraction) × 100%. The percentage of the ceria ENM dose in the capillary rich fraction = (mass amount of cerium in the capillary-rich fraction/mass amount cerium in the total ceria ENM dose) × 100%.

Cerium and gadolinium analysis

Cerium and gadolinium were analyzed by ICP-MS (Agilent 7500cx; Agilent Technologies, Santa Clara, CA), as previously described.[16,33] The method detection limits of Ce and Gd in tissue were 0.013 mg Ce/kg and 0.0004 mg Gd/kg.

Light and electron microscopy

The rats were decapitated at the end of the in situ washout perfusion for brain removal. After bisection, each hemisphere was immediately immersed in a fixative containing 2% paraformaldehyde–2% glutaraldehyde in 0.1 M cacodylate buffer, for 24 hours at 4°C. Tissue samples from the pituitary gland, hippocampus, and choroid plexus were identified with the aid of a dissecting microscope and stored in 0.1 M cacodylate buffer. Samples were cut to approximately 3 mm^3 before being dehydrated in ascending concentrations of ethanol and embedded in Araldite 502 (Electron Microscopy Sciences, Hatfield, PA). After polymerization, the blocks were sectioned at a thickness of one micron and toluidine blue-stained for screening, and selected blocks were sectioned at a thickness of 80 nm for transmission electron microscopy viewing with a Philips CM 10 electron microscope, (FEI Company, Hillsboro, OR), operated at 80 kV.

Data and statistical analysis

The distribution volume, or uptake space (Q), derived from the in situ brain perfusion results, is the amount of brain tissue into which the substrate distributes during a given perfusion duration. $Q_{ceria\ total}$ (mL/g) = ceria ENM in tissue (μg/g)/ceria per volume of perfusate (μg/mL).[34] The mass amount of ceria ENM per gram of brain (μg/g) was also calculated, in order to compare the results of perfusion of the three ceria ENM concentrations. Gd-DTPA uptake space (vascular plus extracellular space) was used to correct the ceria ENM brain uptake space results.[28] $Q_{Gd\text{-}DTPA}$ = Gd-DTPA in tissue (μg/g)/ Gd-DTPA per volume of perfusate (μg/mL). Corrected brain $Q_{ceria\ ENM} = Q_{ceria\ total} - Q_{Gd\text{-}DTPA}$. The corrected mass amount of ceria ENM per gram of brain (μg/g) = ($Q_{ceria\ total} - Q_{Gd\text{-}DTPA}$) (mL/g) × ceria per volume of perfusate (μg/mL). Grubbs' test was used to determine outliers. Two-way ANOVA, followed by Bonferroni multiple comparisons, was used to test for significant differences among the three concentration groups and nine different regions (GraphPad Prism Version 3.00 for Windows; GraphPad Software, San Diego, CA). The percentage of the capillary surface area that would be covered by ceria ENMs was calculated as = (number of ceria ENM particles in the perfused hemisphere × cross-sectional area of a ceria particle) × 100%/rat brain capillary endothelial cell surface area. This was based on the ceria average diameter, the ceria density = 7.132 g/cm^3, and the rat's capillary surface area = 140 cm^2/g brain.[35] All results are reported as mean ± SD.

Results

Nanoparticle characterization

The ceria ENM was polyhedral, and the X-ray diffraction pattern showed the ceria to be highly crystalline. It was face-centered cubic, with corresponding Miller indices of the most common faces of (111), (220), and (311). Evaluation of a number of transmission electron microscopy images (Figure 1A) showed that D_{mean} (average primary particle diameter from number frequency distribution) and standard deviation based on transmission electron microscopy measurements of diameter fitted using lognormal distribution models was 4.6 ± 0.1 nm. Dynamic light scattering results of a representative batch of ceria dispersion showed that 98% of the particles were in the range of 6.7–8.2 nm (Figure 1B). Zeta potential was −53 ± 7 mV at pH ~7.35 in water.

The ceria ENM surface area was 121 m^2/g. The extent of surface citrate coating was ~40%;[19] 5% free cerium ions were in the ceria ENM. After the three filtrations, less than 0.05% of the ceria ENM perfusate was free cerium ions. Ceria ENM was stable in the perfusate at 37°C; no apparent agglomeration was observed from 1 to 230 minutes. The particle size of the ceria ENMs was within ±1 SD after addition of the ceria ENM to the perfusate (Figure 2). In this experiment, the stability of the ceria ENM in the perfusate is crucial for understanding how the ceria ENM interacts with capillary cells and brain tissue.

Flow rate dependency

Comparison of uptake space ($Q_{ceria\ ENM}$) using 15 and 20 mL/minute flow rates did not show a significant flow rate effect on brain ceria ENM uptake in any of the eight brain regions or the choroid plexus. Furthermore, there was no significant

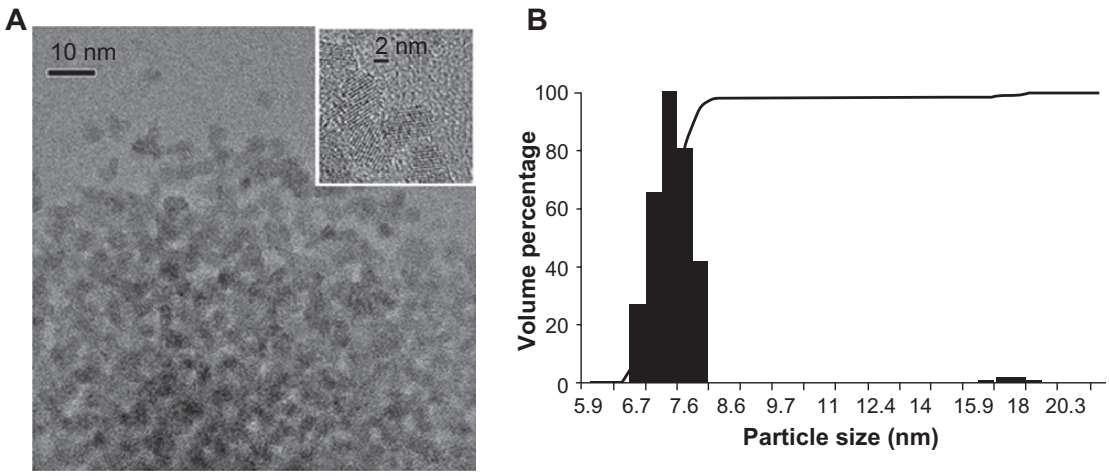

Figure 1 Ceria ENM morphology. (**A**) Ceria ENM imaged using TEM. The insert at the top right shows the crystallinity of the ceria ENM. (**B**) Volume-based particle size distribution for ceria ENM of a representative batch of ceria aqueous dispersion.
Abbreviations: ENM, engineered nanomaterial; TEM, transmission electron microscopy.

difference in the vascular space with these two flow rates or between the control and treated groups. However, the choroid plexus showed a significantly higher vascular space than the eight brain regions (Figure 3). The brain vascular space results were similar to those we measured using [^{14}C]-sucrose.[28] A 20 mL/min flow rate was used for the rest of study.

Ceria ENM uptake

To investigate the 5 nm ceria brain entry rate, its uptake space ($Q_{ceria\ ENM}$) was determined for each brain region for each of the three ceria perfusate concentrations. Figure 4A shows that the uptake space significantly decreased with the increase of ceria ENM concentration in the perfusate. In the 30 μg/mL group, there were no significant differences among the nine regions. However, in the 100 and 500 μg/mL groups, choroid plexus uptake space was significantly higher than in the eight brain regions. In order to compare ceria ENM uptake among the three concentrations, we calculated the mass amount of ceria uptake into the brain as μg/g (Figure 4B). There were no significant differences among the three treatment concentrations. The mass amount of ceria in the choroid plexus uptake space was significantly higher than in the eight brain regions, and it was significantly higher in the 100 and 500 μg/mL groups than in the 30 μg/mL group. The average

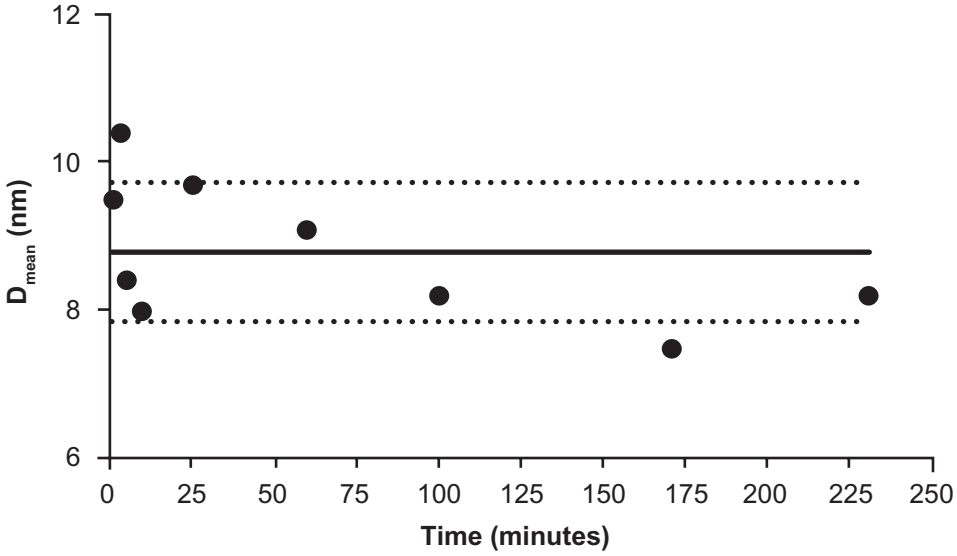

Figure 2 Ceria ENM hydrodynamic diameter in perfusate. Hydrodynamic diameter (intensity weighted average) of ceria ENM in the in situ perfusate, from 1 to 230 minutes (1000 μg/mL at 37°C) after ceria was added to the perfusate.
Notes: Solid circles are DLS data; black solid line is the average of all the data. Dotted lines represent the average diameter ± 1 SD.
Abbreviations: ENM, engineered nanomaterial; DLS, dynamic light scattering; D_{mean}, diameter mean.

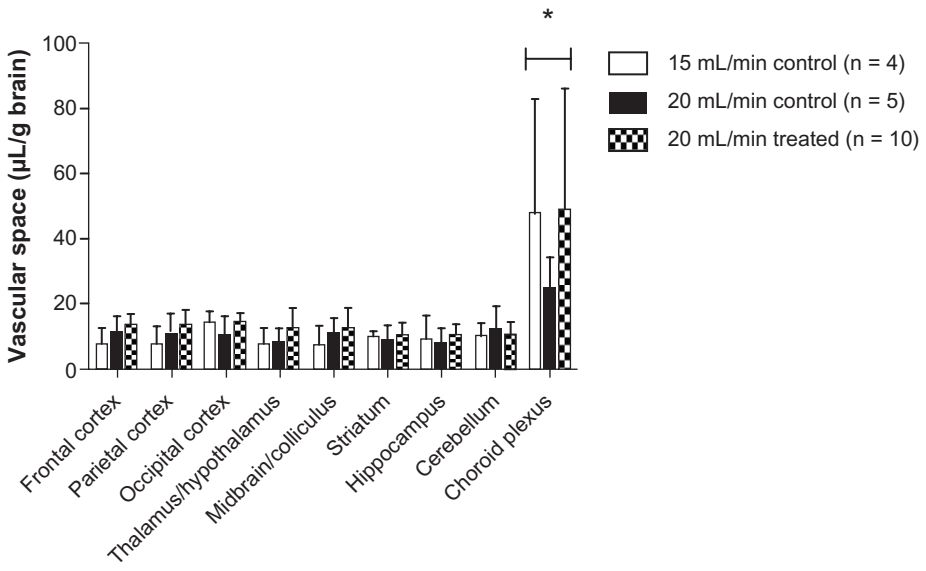

Figure 3 Vascular space of the brain as measured by Gd-DTPA at 15 (n = 4) and 20 (n = 5) mL/minute flow rate in control rats and 20 (n = 10) mL/minute flow rate in 5 nm ceria-treated rats.
Note: *Significantly different from eight brain regions, $P < 0.05$.
Abbreviation: Gd-DTPA, gadolinium-diethylenetriamine pentaacetic acid.

mass amount of ceria per brain hemisphere (0.85 g, excluding choroid plexus) was 4.2 ± 0.7 µg. To verify whether the uptake space of ceria ENM rapidly saturates, ceria uptake space was determined for 30 µg ceria ENM/mL for 20-, 60-, and 120-second perfusion durations. There were significant increases of uptake space to multiple brain regions from 20 to 60 seconds, but no differences between 60 and 120 seconds, suggesting that the uptake space of this ceria ENM saturated between 20 and 60 seconds (Figure 4C). The increased uptake space of the 5 nm ceria ENM showed that the ceria ENM either associated with capillary endothelial cells or entered the brain. In the next step, ceria ENM distribution between cerebral capillary cells and brain parenchyma was determined.

Isolation of cerebral capillaries

Cerebral capillaries were isolated from brain parenchyma to investigate the distribution of ceria ENM between these two fractions. Less than 0.4% of the perfused ceria ENM dose was associated with cerebral capillaries and brain parenchyma. This separation revealed that a great majority of the ceria ENM (99.4% ± 1.1% of the total ceria ENM in the capillary-rich fraction plus brain-rich fraction) was associated with the capillary endothelial cells. Less than 0.003% of the ceria ENM dose was associated with the brain-tissue-rich fraction (Figure 5). These results suggest that most of the 4.2 ± 0.7 µg ceria ENMs in the perfused brain hemisphere were associated with the capillary endothelial cells, and very little ceria ENM passed through the endothelial cells into brain extracellular fluid or brain cells.

Ceria ENM localization using LM and EM

Light and electron microscopy were used to confirm BBB integrity and determine the localization of ceria ENM in the endothelial cells and/or brain parenchyma. Light microscopy examination of the choroid plexus revealed the presence of a cuboidal epithelial cell layer surrounding a core of capillaries, with some surrounding loose connective tissue. There appeared to be no physical injury from exposure to the high perfusate flow rate (Figure 6A). A capillary in the mid-CA1 region of the hippocampus is shown in Figure 6B. The pyramidal cells appear unaffected by in situ perfusion. In the posterior pituitary, capillaries were not affected by the high perfusate flow rate (Figure 6C).

At the ultrastructural level, the endothelial lining of the choroid plexus appeared intact (Figure 7A). The adjacent ependymal cell layer was lined by tightly adhering cells with well-developed surface microvilli creating frond-like processes projecting into the ventricles. Consistent with the high ceria concentration in the choroid plexus, electron-dense ceria ENM agglomerations were observed on the endothelial lining (Figure 7A). Meanwhile, electron-dense nonagglomerated ceria ENM particles adhered to the endothelial lining in the hippocampal vessels (Figure 7B) and the pituitary gland vessels that lacked a BBB (Figure 7C). Ceria ENM associated with the surface of brain capillary endothelial cells.

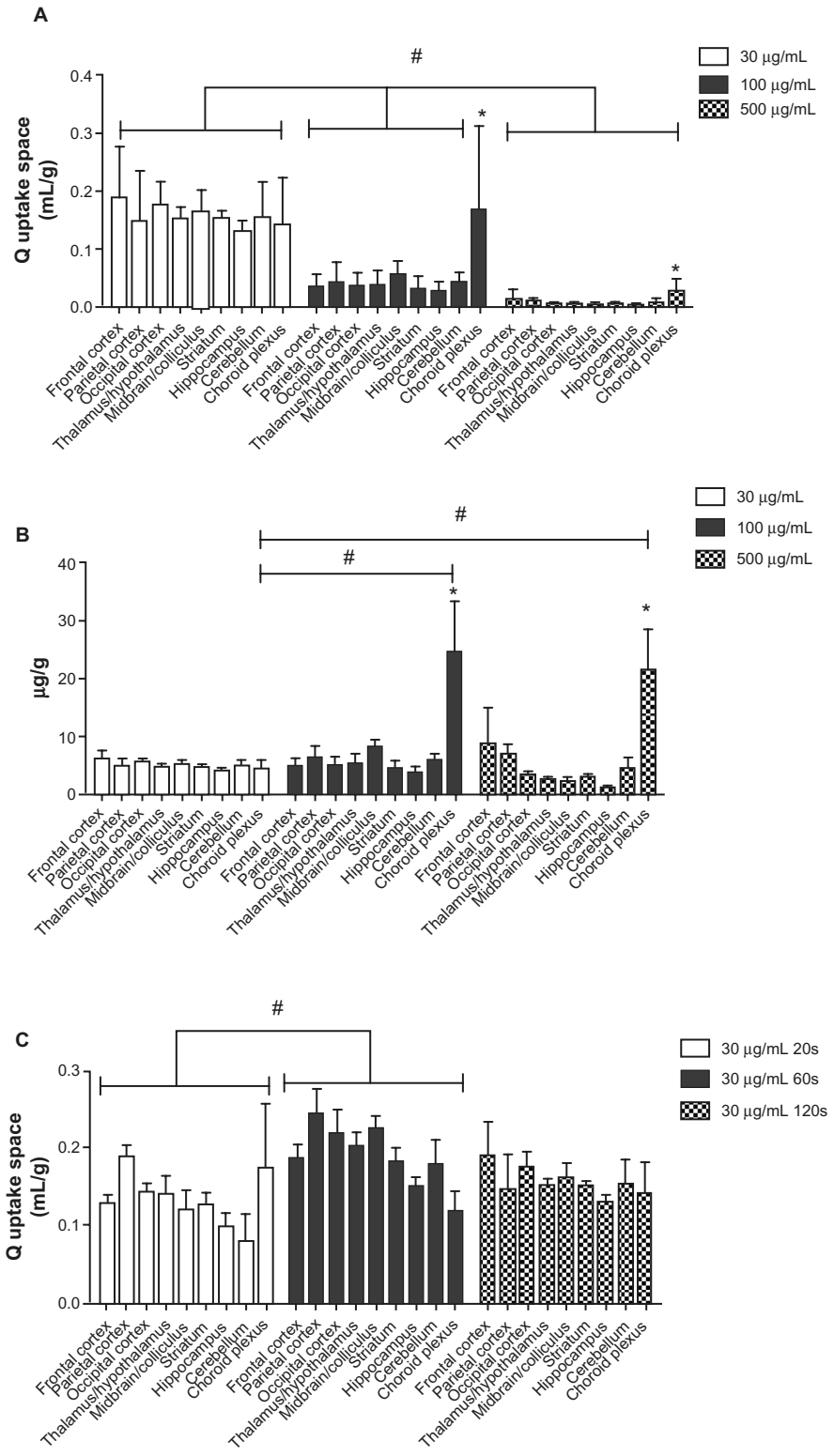

Figure 4 Ceria ENM uptake space at three concentrations and perfusion duration times. Effect of ceria ENM concentration and perfusion duration on its uptake. (**A**) Q uptake space (mL/g) of a 5 nm ceria ENM in eight brain regions and the choroid plexus for three concentrations, at a flow rate of 20 mL/minute, and 120-second perfusion duration. (**B**) Mass amount (µg/g) of 5 nm ceria ENM in eight brain regions and the choroid plexus after brain perfusion with three ceria concentrations, at a flow rate of 20 mL/minute and perfusion duration of 120 seconds. (**C**) Q uptake space (mL/g) of 5 nm ceria ENM in eight brain regions and choroid plexus after 20-, 60-, and 120-second perfusion at 30 µg/mL, at a flow rate of 20 mL/minute.

Notes: (**A**) #Significantly different among three concentration groups, $P < 0.05$; *significantly different compared to the eight brain regions at the same concentration, $P < 0.05$. (**B**) #Significantly different compared to 30 µg/mL concentration group; *significantly different compared to the eight brain regions, $P < 0.05$. (**C**) #Significantly different between 20- and 60-second perfusion duration groups, $P < 0.05$.

Abbreviation: ENM, engineered nanomaterial.

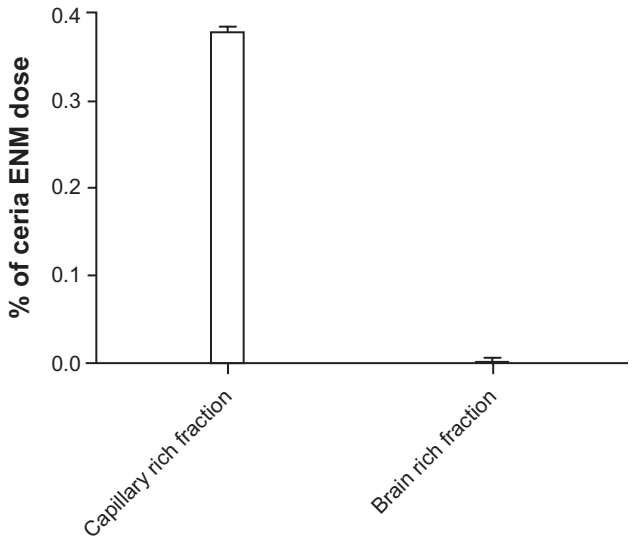

Figure 5 Capillary depletion results. The percentage of the ceria ENM dose in the capillary-rich fraction and brain-rich fraction for 100 μg/mL, at a flow rate of 20 mL/minute, 120-second perfusion duration, followed by 20-second washout.
Abbreviation: ENM, engineered nanomaterial.

No ceria ENM was observed in any brain parenchyma, consistent with our capillary depletion results. The ultrastructural data lend support to the calculation that 2.4% ± 0.4% of the luminal surface area of the capillary endothelial cells would be occupied by the 4.2 ± 0.7 μg ceria ENM per hemisphere measured in our uptake study.

Discussion

The results demonstrate that this ceria ENM did not influence BBB integrity. Perfusate flow rate and ceria ENM concentration did not influence ceria ENM uptake into brain parenchyma, providing evidence of a non-diffusion mechanism. The uptake space of the 5 nm ceria ENM did increase, compared to the vascular space, leading to the conclusion that the 5 nm ceria ENM either associated with capillary endothelial cells or entered the brain. The capillary depletion method showed that most of the ceria ENM associated with the capillary cells. Association of the ceria with the brain endothelial cells was a very rapid process that saturated between 20 and 60 seconds using a flow rate of 20 mL/minute and ceria ENM concentration of 30 μl/mL. Electron microscopy revealed that the ceria ENM associated with the capillary luminal wall, and it was not seen inside the brain capillary endothelial cells.

Prior to recent studies, how metal- or metal oxide-ENMs interact with or cross the brain capillary endothelial cells was poorly understood. One of the issues relevant to how nanomaterials interact with biological membranes is that "what the cell sees" may not be the same as the ENM introduced into the study preparation (eg, cells in culture, intact mammal in this study). Several researchers have shown that ENMs agglomerate in cell culture media.[9,22] In blood, plasma proteins rapidly adsorb to nanoparticle surfaces to form a protein corona that can change the physicochemical properties and influence the fate of ENMs.[20,36,37] It is difficult to interpret some in vitro and in vivo nanoparticle studies, due to their agglomeration in cell culture media and development of the protein corona in blood. In our studies, we used a technique that does not allow the nanoparticles to mix with blood. We determined the size distribution and stability of our ceria ENM in the perfusate from 1 to 230 minutes. The results did not show agglomeration, which was supported by EM images that did not show significant ceria ENM agglomeration in the rat brain. This is the first report of ceria ENM interaction with the BBB, in vivo, under conditions that control ENM chemistry. This research helps us to understand citrate-coated 5 nm ceria brain capillary cell association, potential brain entry, and redistribution. The in situ brain perfusion technique is a good experimental method by which to investigate how physicochemical properties influence the interaction of ENMs with, or their crossing of, the BBB in the absence of major agglomeration and a protein corona. The research helps us understand how certain physicochemical properties influence the ability of ENMs to associate with or cross the BBB for therapeutic application.

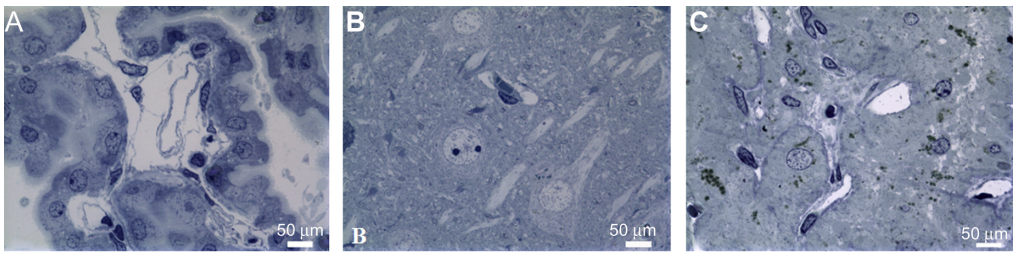

Figure 6 The capillaries in the (**A**) choroid plexus, (**B**) hippocampus (mid-CA1 region), and (**C**) pituitary were not affected by the high perfusate flow rate.
Note: Rats were perfused with 100 μg ceria ENM/mL, at a flow rate of 20 mL/minute, and perfusion duration of 120 seconds.
Abbreviation: ENM, engineered nanomaterial.

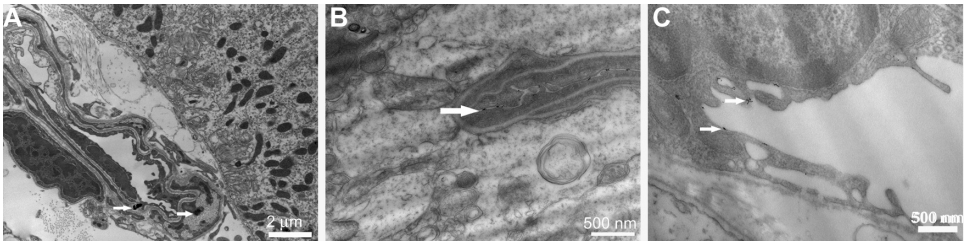

Figure 7 (**A**) A capillary with intact endothelial lining in the choroid plexus containing two ceria ENM agglomerates (arrows). (**B**) A vessel in the hippocampus and (**C**) a vessel from the pituitary gland associated with fine ceria ENM (arrows).
Note: Rats were perfused with 100 µg ceria ENM/mL, at a flow rate of 20 mL/minute, and perfusion duration of 120 seconds.
Abbreviation: ENM, engineered nanomaterial.

Our results showed that most of the ceria ENMs were associated with brain capillary cells rather than brain cells. Several studies reported that metal- and metal oxide-ENMs cross the BBB.[15,16,38,39] Without separating brain capillary cells from brain cells, it is very possible that the ENMs in those studies were associated with endothelial cells rather than entering brain parenchyma. For example, based on ICP-MS results of brain metal content, bovine serum albumin-coated silver-ENM was found in the brain, compared with the control. Signs of silver-induced brain damage were observed; however, EM did not reveal silver-ENMs in the brain.[40] It is possible that the silver-ENMs associated with the BBB and released silver ions to produce the toxicity, rather than being an effect of silver-ENMs. A previous study using the in situ brain perfusion method reported that polymer-based nanoparticles entered the central nervous system within 60 seconds, without influencing BBB integrity. However, the researchers did not separate the capillary cells from the brain parenchyma. They showed an uptake space similar to results we obtained at 20 and 60 seconds. Capillary association also may contribute to their brain uptake space.[41] Our previous studies showed only 0.02% of a 5 nm ceria dose in the brain 1 hour after IV infusion. However, we did not observe any 5 nm ceria ENM in the brain tissue.[19] In light of the results in this paper, the 0.02% ceria in the brain may be ceria ENM in blood and associated with capillary cells. In this study, brain association (0.383% of the ceria ENM dose) using in situ perfusion is 19 times higher than our previous report of ceria ENM in the brain (0.02% of the ceria dose) 1 hour after IV infusion. The different timelines (in the prior study, brain samples were obtained 1 hour after completion of ceria infusion; in the present study, the samples were obtained immediately after completion of ceria perfusion) and routes (IV versus intra-carotid artery) contributed to the differences in brain ceria ENM. In the present study using in situ brain perfusion, ceria ENM did not mix with blood and avoided first-pass clearance. After IV administration, ceria ENM agglomerated in the blood, and protein corona formation changed its physicochemical properties, resulting in rapid clearance by the mononuclear phagocyte system.[21,26] Ceria ENM may associate with brain capillary cells during a 120-second perfusion and dissociate later. The above reasons may explain the high brain capillary/ceria ENM association, compared with our previous IV infusion study.

Our EM results showed that most of the ceria ENM is on the luminal surface of brain capillary cells rather than inside these cells. Brain capillary cell association with this negatively charged ceria ENM is in agreement with a previous kinetic study that reported a negatively charged nanoparticle associated with the cell surface, within seconds, by Langmuir adsorption through electrostatic interaction.[42] After surface adsorption, the next step may be dissociation and redistribution or cell internalization. The time course of cell internalization of metal oxide nanoparticles is still under investigation. Anionic iron oxide-ENMs attached onto the cell membrane of HeLa cells immediately after ENM introduction to the cells. Early endocytic-coated vesicles were observed at 10 minutes.[42] Most of the literature we are aware of showed cell line- and material-dependent ENM internalization half lives of more than a few minutes in vitro and in vivo.[42–46] In three different cancer cells, 14, 50, and 74 nm gold nanoparticles had uptake half-lives of more than 1 hour.[43] Flux of cationic arginine–vasopressin nanoparticles across the BBB started at 15 minutes through absorptive-mediated endocytosis in mice.[45] Because of the nature of the in situ perfusion technique, perfusion duration in the present study was not greater than 120 seconds.[34] More research is needed to understand what happens after the ceria ENMs interact with brain capillary cells. However, no matter what does happen, it is very important to know the rate and extent of cell surface adsorption, as it is the initial step for ENM cell uptake and potential redistribution back into the blood.

In this study, capillary depletion results showed ceria ENM associated with brain endothelial cells. Electron

microscopy failed to find any 5 nm ceria in brain parenchyma; however, nonagglomerated ceria ENM was observed to associate with the luminal wall of brain capillary endothelial cells. Assuming that all of the ceria associated with the capillary surface without any agglomeration, and based on the mass of ceria ENM we observed in the rat brain after arterial ceria ENM perfusion, our calculation showed that 2.4% ± 0.4% of the brain capillary surface area might be covered by the ceria ENM. We think that the 4.2 ± 0.7 μg of ceria ENM per brain hemisphere seen in the present study might contribute to ceria ENM redistribution or sustained release back into the blood. Ceria ENM dissociation from the brain capillary luminal wall over time may provide an explanation for findings in our pharmacokinetic study, wherein the circulating blood level of two sizes of ceria ENMs increased from 2 to 4 hours after completion of their IV infusion, which cannot be explained using conventional pharmacokinetics.[26] A similar increase of ENM in blood within the first 2 hours after its IV administration has been reported for quantum dots; however, explanation of the increase was not discussed in these reports.[47,48] ENMs that associate with, and subsequently disassociate from, the vascular wall might provide an explanation. Another study showed that 100–200 nm ceria ENMs (primary size, 3–5 nm) were observed on the luminal surface of mouse tail veins 30 days post-IV injection.[49] It is not known if these agglomerated ceria nanoparticles were from original association with the blood vessel or from redistribution over time. In general, our results showed that ENMs can associate with capillary cells, which may contribute to nanoparticle redistribution back into the blood.

This is the first study to report that a ceria ENM has a higher concentration in the choroid plexus compared with brain regions. Our vascular space results, measured by Gd-DTPA, showed that the choroid plexus has a larger vascular space than brain tissues. The choroid plexus showed a significantly higher uptake space compared with brain regions in the 100 and 500 μg/mL concentration groups, but not in the 30 μg/mL group. The choroid plexus uptake space did not change between the 100 and 500 μg/mL groups. Little is known about how metal oxide nanoparticles interact with the choroid plexus. The choroid plexus has larger surface area per mass, a leakier epithelial barrier, and different tight junction proteins and transport protein expression compared to cerebral endothelium.[50,51] The fundamental differences between the choroidal epithelium and the cerebral endothelium may influence the ceria ENM association sites and determine the ceria ENM saturation concentration. Ceria agglomerates (Figure 7) were observed in the choroid plexus, compared to primary fine ceria ENM on the surface of the brain endothelial cells, providing evidence that ceria ENM may associate with the choroid plexus differently than the BBB, leading to higher concentrations in the choroid plexus. Previous research showed that the choroid plexus sequesters metal ions rapidly, and that their concentrations were more than ten times higher than other brain regions.[28,52] Some polymer nanoparticles showed similar results as the present study. Poly (d,l-lactide-co-glycolide) nanoparticles showed a high concentration in the choroid plexus.[53] The choroid plexus is considered a potential region to retain nanoparticles,[54] and a pathway to enter the central nervous system.[51,55] Our results provide the first evidence that ceria ENMs interact significantly with the choroid plexus; this information is very important for toxicity concerns and therapeutic applications.

Conclusion

Brain uptake of a 5 nm ceria ENM was flow rate- and perfusion concentration-independent, showing that diffusion was not mediating its association with brain tissue. The ceria ENM concentration was significantly higher in the choroid plexus than in eight brain regions. Brain ceria ENM association was a very rapid process that reached saturation between 20 and 60 seconds. The capillary depletion method showed that the ceria ENM was predominantly associated with the brain capillary cells rather than with brain parenchyma. Furthermore, EM showed that most of the ceria ENM associated with the luminal surface of brain endothelial cells, rather than entering the cells. This research provides the first data on the kinetics of ceria ENM interaction with the BBB and choroid plexus. Ceria ENM capillary cell surface association also provides a site from which it can dissociate, redistribute, or enter the capillary cells. This information will be important for the design of ceria ENMs as a therapeutic agent, as well as for a comprehensive toxicology assessment.

Acknowledgments

This work was supported by United States Environmental Protection Agency Science to Achieve Results [grant number RD-833772]. Although the research described in this article has been funded wholly or in part by the United States Environmental Protection Agency through STAR Grant RD-833772, it has not been subjected to the Agency's required peer and policy review and, therefore, it does not necessarily reflect the views of the Agency, and no official endorsement should be inferred.

Disclosure

The authors report no conflicts of interest in this work.

References

1. Tarnuzzer RW, Colon J, Patil S, Seal S. Vacancy engineered ceria nanostructures for protection from radiation-induced cellular damage. *Nano Lett*. 2005;5(12):2573–2577.
2. Schubert D, Dargusch R, Raitano J, Chan SW. Cerium and yttrium oxide nanoparticles are neuroprotective. *Biochem Biophys Res Commun*. 2006;342(1):86–91.
3. Das M, Patil S, Bhargava N, et al. Auto-catalytic ceria nanoparticles offer neuroprotection to adult rat spinal cord neurons. *Biomaterials*. 2007;28(10):1918–1925.
4. Xia T, Kovochich M, Liong M, et al. Comparison of the mechanism of toxicity of zinc oxide and cerium oxide nanoparticles based on dissolution and oxidative stress properties. *ACS Nano*. 2008;2(10):2121–2134.
5. Estevez AY, Pritchard S, Harper K, et al. Neuroprotective mechanisms of cerium oxide nanoparticles in a mouse hippocampal brain slice model of ischemia. *Free Radic Biol Med*. 2011;51(6):1155–1163.
6. Amin KA, Hassan MS, Awad el-ST, Hashem KS. The protective effects of cerium oxide nanoparticles against hepatic oxidative damage induced by monocrotaline. *Int J Nanomedicine*. 2011;6:143–149.
7. Chen J, Patil S, Seal S, McGinnis JF. Rare earth nanoparticles prevent retinal degeneration induced by intracellular peroxides. *Nat Nanotechnol*. 2006;1(2):142–150.
8. Singh N, Cohen CA, Rzigalinski BA. Treatment of neurodegenerative disorders with radical nanomedicine. *Ann N Y Acad Sci*. 2007;1122:219–230.
9. Eom HJ, Choi J. Oxidative stress of CeO_2 nanoparticles via p38-Nrf-2 signaling pathway in human bronchial epithelial cell, Beas-2B. *Toxicol Lett*. 2009;187(2):77–83.
10. Heckert EG, Seal S, Self WT. Fenton-like reaction catalyzed by the rare earth inner transition metal cerium. *Environ Sci Technol*. 2008;42(13):5014–5019.
11. Nalabotu SK, Kolli MB, Triest WE, et al. Intratracheal instillation of cerium oxide nanoparticles induces hepatic toxicity in male Sprague-Dawley rats. *Int J Nanomedicine*. 2011;6:2327–2335.
12. Bernacki J, Dobrowolska A, Nierwinska K, Malecki A. Physiology and pharmacological role of the blood–brain barrier. *Pharmacol Rep*. 2008;60(5):600–622.
13. Barbu E, Molnar E, Tsibouklis J, Gorecki DC. The potential for nanoparticle-based drug delivery to the brain: overcoming the blood–brain barrier. *Expert Opin Drug Deliv*. 2009;6(6):553–565.
14. Kreuter J, Gelperina S. Use of nanoparticles for cerebral cancer. *Tumori*. 2008;94(2):271–277.
15. Chen L, Yokel RA, Hennig B, Toborek M. Manufactured aluminum oxide nanoparticles decrease expression of tight junction proteins in brain vasculature. *J Neuroimmune Pharmacol*. 2008;3(4):286–295.
16. Yokel RA, Florence RL, Unrine JM, et al. Biodistribution and oxidative stress effects of a systemically-introduced commercial ceria engineered nanomaterial. *Nanotoxicology*. 2009;3(3):234–248.
17. Sonavane G, Tomoda K, Makino K. Biodistribution of colloidal gold nanoparticles after intravenous administration: effect of particle size. *Colloids Surf B Biointerfaces*. 2008;66(2):274–280.
18. He X, Zhang H, Ma Y, et al. Lung deposition and extrapulmonary translocation of nano-ceria after intratracheal instillation. *Nanotechnology*. 2010;21(28):285103.
19. Hardas SS, Butterfield DA, Sultana R, et al. Brain distribution and toxicological evaluation of a systemically delivered engineered nanoscale ceria. *Toxicol Sci*. 2010;116(2):562–576.
20. Deng ZJ, Mortimer G, Schiller T, Musumeci A, Martin D, Minchin RF. Differential plasma protein binding to metal oxide nanoparticles. *Nanotechnology*. 2009;20(45):455101.
21. Yokel RA, Tseng MT, Dan M, et al. Biodistribution, biopersistence and associated toxicity of ceria engineered nanomaterial. *Nanomed Nanotech Biol Med*. Submitted.
22. Wang J, Rahman MF, Duhart HM, et al. Expression changes of dopaminergic system-related genes in PC12 cells induced by manganese, silver, or copper nanoparticles. *Neurotoxicology*. 2009;30(6):926–933.
23. Nel AE, Madler L, Velegol D, et al. Understanding biophysicochemical interactions at the nano-bio interface. *Nat Mater*. 2009;8(7):543–557.
24. Walczyk D, Bombelli FB, Monopoli MP, Lynch I, Dawson KA. What the cell "sees" in bionanoscience. *J Am Chem Soc*. 2010;132(16):5761–5768.
25. Mandzy N, Grulke E, Druffel T. Breakage of TiO2 agglomerates in electrostatically stabilized aqueous dispersions. *Powder Technol*. 2005;160(2):121–126.
26. Dan M, Wu P, Grulke EA, Graham UM, Unrine JM, Yokel RA. Ceria-engineered nanomaterial distribution in, and clearance from, blood: size matters. *Nanomedicine (Lond)*. 2012;7(1):95–110.
27. Bronen RA, Sze G. Magnetic resonance imaging contrast agents: theory and application to the central nervous system. *J Neurosurg*. 1990;73(6):820–839.
28. Crossgrove JS, Allen DD, Bukaveckas BL, Rhineheimer SS, Yokel RA. Manganese distribution across the blood–brain barrier. I. Evidence for carrier-mediated influx of managanese citrate as well as manganese and manganese transferrin. *Neurotoxicology*. 2003;24(1):3–13.
29. Crossgrove JS, Yokel RA. Manganese distribution across the blood–brain barrier. III. The divalent metal transporter-1 is not the major mechanism mediating brain manganese uptake. *Neurotoxicology*. 2004;25(3):451–460.
30. Crossgrove JS, Yokel RA. Manganese distribution across the blood–brain barrier. IV. Evidence for brain influx through store-operated calcium channels. *Neurotoxicology*. 2005;26(3):297–307.
31. Smith QR. Brain perfusion systems for studies of drug uptake and metabolism in the central nervous system. *Pharm Biotechnol*. 1996;8:285–307.
32. Triguero D, Buciak J, Pardridge WM. Capillary depletion method for quantification of blood–brain barrier transport of circulating peptides and plasma proteins. *J Neurochem*. 1990;54(6):1882–1888.
33. Hardas SS, Butterfield DA, Sultana R, et al. Brain distribution and toxicological evaluation of a systemically delivered engineered nanoscale ceria. *Toxicol Sci.* 2010;116(2):562–576.
34. Takasato Y, Rapoport SI, Smith QR. An in situ brain perfusion technique to study cerebrovascular transport in the rat. *Am J Physiol*. 1984;247 (3 Pt 2):H484–H493.
35. Crone C, Levitt DG. *Capillary permeability to small solutes. In: Handbook of Physiology. The Cardiovascular System. Microcirculation.* Bethesda, MD: Am Physiol Soc; 1984.
36. Owens DE, Peppas NA. Opsonization, biodistribution, and pharmacokinetics of polymeric nanoparticles. *Int J Pharm*. 2006;307(1):93–102.
37. Li M, Al-Jamal KT, Kostarelos K, Reineke J. Physiologically based pharmacokinetic modeling of nanoparticles. *ACS Nano*. 2010;4(11):6303–6317.
38. De Jong WH, Hagens WI, Krystek P, Burger MC, Sips AJ, Geertsma RE. Particle size-dependent organ distribution of gold nanoparticles after intravenous administration. *Biomaterials*. 2008;29(12):1912–1919.
39. Lockman PR, Koziara JM, Mumper RJ, Allen DD. Nanoparticle surface charges alter blood–brain barrier integrity and permeability. *J Drug Target*. 2004;12(9–10):635–641.
40. Garza-Ocanas L, Ferrer DA, Burt J, et al. Biodistribution and long-term fate of silver nanoparticles functionalized with bovine serum albumin in rats. *Metallomics*. 2010;2(3):204–210.
41. Koziara JM, Lockman PR, Allen DD, Mumper RJ. In situ blood–brain barrier transport of nanoparticles. *Pharm Res*. 2003;20(11):1772–1778.

42. Wilhelm C, Gazeau F, Roger J, Pons JN, Bacri JC. Interaction of anionic superparamagnetic nanoparticles with cells: kinetic analyses of membrane adsorption and subsequent internalization. *Langmuir*. 2002;18(21):8148–8155.
43. Chithrani BD, Chan WC. Elucidating the mechanism of cellular uptake and removal of protein-coated gold nanoparticles of different sizes and shapes. *Nano Lett*. 2007;7(6):1542–1550.
44. Serda RE, Gu J, Burks JK, Ferrari K, Ferrari C, Ferrari M. Quantitative mechanics of endothelial phagocytosis of silicon microparticles. *Cytometry A*. 2009;75(9):752–760.
45. Tanabe S, Shimohigashi Y, Nakayama Y, et al. In vivo and in vitro evidence of blood–brain barrier transport of a novel cationic arginine–vasopressin fragment 4–9 analog. *J Pharmacol Exp Ther*. 1999;290(2):561–568.
46. Kang YS, Pardridge WM. Brain delivery of biotin bound to a conjugate of neutral avidin and cationized human albumin. *Pharm Res*. 1994;11(9):1257–1264.
47. Al-Jamal WT, Al-Jamal KT, Cakebread A, Halket JM, Kostarelos K. Blood circulation and tissue biodistribution of lipid – quantum dot (L-QD) hybrid vesicles intravenously administered in mice. *Bioconjug Chem*. 2009;20(9):1696–1702.
48. Fischer HC, Liu L, Pang KS, Chan WCW. Pharmacokinetics of nanoscale quantum dots: in vivo distribution, sequestration, and clearance in the rat. *Adv Funct Mater*. 2006;16(10):1299–1305.
49. Hirst SM, Karakoti AS, Tyler RD, Sriranganathan N, Seals S, Reilly CM. Anti-inflammatory properties of cerium oxide nanoparticles. *Small*. 2009;5(24):2848–2856.
50. Strazielle N, Ghersi-Egea JF. Choroid plexus in the central nervous system: biology and physiopathology. *J Neuropathol Exp Neurol*. 2000;59(7):561–574.
51. Redzic Z. Molecular biology of the blood–brain and the blood–cerebrospinal fluid barriers: similarities and differences. *Fluids Barriers CNS*. 2011;8(1):3.
52. Zheng W. Toxicology of choroid plexus: Special reference to metal-induced neurotoxicities. *Microsc Res Tech.* 2001;52(1):89–103.
53. Wang ZH, Wang ZY, Sun CS, Wang CY, Jiang TY, Wang SL. Trimethylated chitosan-conjugated PLGA nanoparticles for the delivery of drugs to the brain. *Biomaterials*. 2010;31(5):908–915.
54. Räty JK, Liimatainen T, Wirth T, et al. Magnetic resonance imaging of viral particle biodistribution in vivo. *Gene Ther*. 2006;13(20):1440–1446.
55. Salmaso S, Pappalardo JS, Sawant RR, et al. Targeting glioma cells in vitro with ascorbate-conjugated pharmaceutical nanocarriers. *Bioconjug Chem*. 2009;20(12):2348–2355.

Supplementary materials

Materials and methods

Materials

The chemicals used to prepare the ceria engineered nanomaterials (ENMs) have been described.[1] Cerium chloride heptahydrate (#228931, 99.9% metal basis; Sigma-Aldrich, St Louis, MO), ammonium hydroxide (Thermo Fisher Scientific, Waltham, MA; #3256, ACS, 28%–30%), deionized ultra filtered water (Thermo Fisher Scientific; #W2-20), and citric acid monohydrate (EMD Millipore, Billerica, MA; #CX1725-1, GR ACS) were used without further purification. All other chemicals were purchased from Sigma-Aldrich unless otherwise noted.

Ceria ENM synthesis

Synthesis of the 5 nm ceria ENM was described.[2] It was synthesized using a hydrothermal method[3] that produces monodisperse nanoparticles directly in the reactor. Typically, a 20 mL aqueous mixture of 0.5 M (0.01 mol) cerium chloride and 0.5 M (0.01 mol) citric acid was added to 20 mL of 3 M ammonium hydroxide. The latter was in excess of what was needed for complete reaction of the cerium chloride to cerium hydroxide. After stirring for 24 hours at 50°C, the solution was transferred to a Teflon-lined, stainless steel bomb, and heated at 80°C for 24 hours to complete the reaction. The ceria ENMs were citrate coated (capped) to improve their dispersity in water to stabilize dispersion through electrostatic repulsion and prevent the agglomeration seen with uncoated ceria that occurs in high ionic strength solutions, such as blood.[4–6] Citrate was selected because: it is a commonly used surface coating agent for ENMs to inhibit agglomeration (eg, National Institute of Standards of Technology reference materials 8011, 8012, and 8013 [NIST, Gaithersburg, MD]); it is a component of blood (present at ~100 μM in humans); it might coat bare ENMs circulating in blood; it has been shown to have no effect on erythrocyte response to silver-ENMs; and citrate-coated ENMs interact strongly with proteins, resulting in the rapid opsonization that occurs when ENMs enter blood.[7–9]

Ceria ENM characterization

The physicochemical properties of the ceria ENMs were determined in our laboratories. Most of the methods have been reported.[1] Primary particle size distributions were determined by transmission electron microscopy (TEM) and scanning transmission electron microscopy (200-keV field emission analytical transmission electron microscope, JEM-2010F; JEOL, Tokyo, Japan). From the individual primary particle sizes measured from TEM images, number frequency cumulative distributions were constructed. These cumulative distributions were best described by log-normal distribution models, characterized by a sample mean and its standard deviation. All of these data sets were well described by a single monomodal distribution; that is, one continuous distribution was observed, and no significant secondary or tertiary peaks were noted. The reported average diameter of each sample was $D_{ave} = \exp(\mu)$, where μ is the mean of the log-normal probability distribution and the reported standard deviation is the value from the fit of the log-normal distribution to the data. For each sample, number-based differential frequency distributions were constructed using the model coefficients. The particle size distributions for each batch of as-synthesized ceria aqueous dispersion were determined using dynamic light scattering (DLS; 90Plus NanoParticle Size Distribution Analyzer; Brookhaven Instruments Corporation, Holtsville, NY). Zeta potential of the ceria dispersion as infused into the rat was estimated from electrophoretic mobility measurements, using a Zetasizer nanoZS with a typical ceria concentration ~0.02 wt% (Malvern Instruments, Worcestershire, UK). Because the particles had hydrodynamic diameters < 200 nm, the Hückel approximation was used to calculate zeta potential from electrophoretic mobility. The surface area of the dried powder was determined using a Brunauer–Emmett–Teller surface area analyzer (Micromeritics Instrument Corporation, Norcross, GA). Thermogravimetric analysis (TGA7 Analyzer; PerkinElmer, Waltham, MA) was then performed to investigate the weight loss of citrate-coated ceria nanoparticles (NPs) over a 150°C–300°C temperature range, during which decomposition of citric acid occurs. The extent of citrate surface coating was estimated based on the assumption that all the ceria NPs were spherical and of uniform size.

References

1. Dan M, Wu P, Grulke EA, Graham UM, Unrine JM, Yokel RA. Ceria-engineered nanomaterial distribution in, and clearance from, blood: size matters. *Nanomedicine (Lond)*. 2012;7(1):95–110.
2. Hardas SS, Butterfield DA, Sultana R, et al. Brain distribution and toxicological evaluation of a systemically delivered engineered nanoscale ceria. *Toxicol Sci*. 2010;116(2):562–576.
3. Masui T, Hirai H, Imanaka N, Adachi G, Sakata T, Mori H. Synthesis of cerium oxide nanoparticles by hydrothermal crystallization with citric acid. *J Mater Sci Lett*. 2002;21(6):489–491.
4. Xia T, Kovochich M, Liong M, et al. Comparison of the mechanism of toxicity of zinc oxide and cerium oxide nanoparticles based on dissolution and oxidative stress properties. *ACS Nano*. 2008;2(10):2121–2134.

5. Cao T, Yang T, Gao Y, Yang Y, Hu H, Li F. Water-soluble NaYF4:Yb/Er upconversion nanophosphors: synthesis, characteristics and application in bioimaging. *Inorg Chem Commun*. 2010;13(3):392–394.
6. Frasca G, Gazeau F, Wilhelm C. Formation of a three-dimensional multicellular assembly using magnetic patterning. *Langmuir.* 2009;25(4):2348–2354.
7. Brewer SH, Glomm WR, Johnson MC, Knag MK, Franzen S. Probing BSA binding to citrate-coated gold nanoparticles and surfaces. *Langmuir.* 2005;21(20):9303–9307.
8. Choi J, Reipa V, Hitchins VM, Goering PL, Malinauskas RA. Physicochemical characterization and in vitro hemolysis evaluation of silver nanoparticles *Toxicol Sci.* 2011;123(1):133–143.
9. Viota JL, Rudzka K, Trueba Á, Torres-Aleman I, Delgado ÁV. Electrophoretic characterization of insulin growth factor (IGF-1) functionalized magnetic nanoparticles. *Langmuir*. 2011;27(10):6426–6432.
10. Packer AP, Lariviere D, Li C, et al. Validation of an inductively coupled plasma mass spectrometry (ICP-MS) method for the determination of cerium, strontium, and titanium in ceramic materials used in radiological dispersal devices (RDDs). *Anal Chim Acta*. 2007;588(2):166–172.
11. Yokel RA, Florence RL, Unrine JM, et al. Biodistribution and oxidative stress effects of a systemically-introduced commercial ceria engineered nanomaterial. *Nanotoxicology*. 2009;3(4):234–248.